A Perfectly Matched Layer for the 3-D Wave Equation in the Time Domain

Yotka Rickard, *Student Member, IEEE*, Natalia Georgieva, *Member, IEEE*, and Wei-Ping Huang, *Senior Member, IEEE*

***Abstract*—In this letter, a three-dimensional (3-D) PML for the 3-D scalar wave equation is proposed for applications in practical finite difference time-domain schemes such as the time-domain wave-potential (TDWP) technique and the time-domain scalar wave equation approaches to the analysis of optical waveguides. The theoretical formulation is based on the stretched coordinates approach. It is shown that this PML is suitable for the termination of open problems as well as for port terminations in high-frequency circuit problems. New PML conductivity profile is proposed, which offers lower reflections in a wider frequency band in comparison with the commonly used profiles.**

***Index Terms*—Absorbing boundary conditions (ABC), finite-difference time-domain (FDTD) methods, perfectly matched layer (PML), wave equation (WE).**

I. Introduction

THE perfectly matched layer (PML) introduced by Berenger [1], [2] is widely recognized as one of the most efficient numerical absorbers used in time-domain electromagnetic (EM) solvers. It has been used in conjunction with the finite difference time-domain (FDTD) algorithm, as well as with the finite element time-domain (FETD) method. PML ABCs have been also developed for most frequency-domain techniques, such as the finite element method (FEM), the finite-difference frequency-domain (FDFD) method and the beam propagation method (BPM) [3]–[6].

Recently, the one-directional PML absorbing boundary condition (ABC) has been applied to terminate one of the ports in a dielectric-slab waveguide problem solved in terms of the two-dimensional (2-D) scalar wave equation in the time domain [7]. In this paper, we extend and validate the method proposed in [7] to a general three-dimensional (3-D) PML for the 3-D wave equation in the time domain. In the most recent years, the scalar wave equations are being applied in time-domain computational algorithms not only for optical waveguides and structures, but also in the microwave and millimeter-wave structure analysis [8], [9]. These new algorithms require a reliable and efficient ABC, which can handle both open problems (i.e., radiation and scattering) and problems involving port terminations (high-frequency circuit problems). The proposed PML is applicable to the termination of both lossless and lossy media. Here, the first applications in loss-free problems are demonstrated.

Manuscript received September 11, 2001; revised February 15, 2002. The review of this letter was approved by Associated Editor Dr. Rüdiger Vahldieck.

The authors are with the Department of Electrical and Computer Engineering, McMaster University, Hamilton, ON L8S 4KA, Canada.

Publisher Item Identifier S 1531-1309(02)04477-X.

II. Derivation of the PML Equations

We start with the lossy wave equation (WE) in the time domain [8]

$$\nabla^2\vec{A}-\mu\varepsilon\partial_{tt}^2\vec{A}-(\mu\sigma+\varepsilon\sigma_m)\,\partial_t\vec{A}-\sigma\sigma_m\vec{A}=-\mu\vec{J}. \quad (1)$$

Here, ∂_{tt}^2 and ∂_t denote the second-order and the first-order derivatives with respect to time. Using the stretched coordinate approach [10], we introduce the stretched-coordinate complex variables s_x, s_y, s_z along the three Cartesian coordinates in the Laplacian

$$\nabla_s^2=s_x^{-1}\partial_x\left(s_x^{-1}\partial_x\right)+s_y^{-1}\partial_y\left(s_y^{-1}\partial_y\right)+s_z^{-1}\partial_z\left(s_z^{-1}\partial_z\right) \quad (2)$$

where $s_\xi=\alpha_\xi+\sigma_\xi/(j\omega\varepsilon)$, $\xi=x,y,z$. The WE in (1) is then mapped into the frequency domain

$$\nabla_s^2\tilde{\vec{A}}-\mu\varepsilon\,(j\omega)^2\,\tilde{\vec{A}}-(\mu\sigma+\varepsilon\sigma_m)\,j\omega\tilde{\vec{A}}-\sigma\sigma_m\tilde{\vec{A}}=-\mu\tilde{\vec{J}}. \quad (3)$$

Six auxiliary variables are introduced in a fashion similar to that in [7]

$$\begin{aligned}
j\omega\tilde{\vec{X}}_1&=s_x^{-1}\partial_x\tilde{\vec{A}};\quad j\omega\tilde{\vec{X}}_2=s_x^{-1}\partial_x\left(j\omega\tilde{\vec{X}}_1\right)\\
j\omega\tilde{\vec{Y}}_1&=s_y^{-1}\partial_y\tilde{\vec{A}};\quad j\omega\tilde{\vec{Y}}_2=s_y^{-1}\partial_y\left(j\omega\tilde{\vec{Y}}_1\right)\\
j\omega\tilde{\vec{Z}}_1&=s_z^{-1}\partial_z\tilde{\vec{A}};\quad j\omega\tilde{\vec{Z}}_2=s_z^{-1}\partial_z\left(j\omega\tilde{\vec{Z}}_1\right).
\end{aligned} \quad (4)$$

The mapped frequency-domain WE now becomes

$$\begin{aligned}
\mu\varepsilon(j\omega)^2\tilde{\vec{A}}+(\mu\sigma+\varepsilon\sigma_m)\,j\omega\tilde{\vec{A}}+\sigma\sigma_m\tilde{\vec{A}}\\
=j\omega\tilde{\vec{X}}_2+j\omega\tilde{\vec{Y}}_2+j\omega\tilde{\vec{Z}}_2+\mu\tilde{\vec{J}}
\end{aligned} \quad (5)$$

which can be mapped back into the time domain as

$$\begin{aligned}
\mu\varepsilon\partial_{tt}^2\vec{A}+(\mu\sigma+\varepsilon\sigma_m)\,\partial_t\vec{A}+\sigma\sigma_m\vec{A}\\
=\partial_t\vec{X}_2+\partial_t\vec{Y}_2+\partial_t\vec{Z}_2+\mu\vec{J}.
\end{aligned} \quad (6)$$

The auxiliary variables in the time domain are calculated according to the equations in (4), which are also mapped back into the time domain

$$\begin{aligned}
\alpha_x\partial_t\vec{X}_1+\left(\frac{\sigma_x}{\varepsilon}\right)\vec{X}_1&=\partial_x\vec{A};\quad \alpha_x\partial_t\vec{X}_2+\left(\frac{\sigma_x}{\varepsilon}\right)\vec{X}_2=\partial_{xt}^2\vec{X}_1\\
\alpha_y\partial_t\vec{Y}_1+\left(\frac{\sigma_y}{\varepsilon}\right)\vec{Y}_1&=\partial_y\vec{A};\quad \alpha_y\partial_t\vec{Y}_2+\left(\frac{\sigma_y}{\varepsilon}\right)\vec{Y}_2=\partial_{yt}^2\vec{Y}_1\\
\alpha_z\partial_t\vec{Z}_1+\left(\frac{\sigma_z}{\varepsilon}\right)\vec{Z}_1&=\partial_z\vec{A};\quad \alpha_z\partial_t\vec{Z}_2+\left(\frac{\sigma_z}{\varepsilon}\right)\vec{Z}_2=\partial_{zt}^2\vec{Z}_1.
\end{aligned} \quad (7)$$

III. PML Conductivity Profiles

The profile of the PML variables is of crucial importance to the performance of the numerical absorber. Initially, we have implemented a variety of profiles already available in the literature, such as in [1], [11], and [12]. However, the PML is now integrated with the wave equation where one no longer deals with the field vectors. Importing existing PMLs directly into the wave equation algorithm does not produce the desired absorption. The PML profile has to be modified and optimized. The best performance is achieved with the following new modification of the PML conductivity σ, which is now proposed to be of one order higher than the order of the loss factor α

$$\sigma_i(\rho) = \sigma_{\max}\left(\frac{\rho}{\delta}\right)^{n+1} = \frac{(n+2)\varepsilon_0 c \ln\left(R_0^{-1}\right)}{2\delta}\left(\frac{\rho}{\delta}\right)^{n+1}, i = x, y, z \quad (8)$$

$$\alpha_i(\rho) = 1 + \varepsilon_{\max}\left(\frac{\rho}{\delta}\right)^{n}, \rho \in [0, \delta], i = x, y, z. \quad (9)$$

Here, δ is the PML thickness, ρ is the depth in the PML, R_0 is the chosen reflection coefficient at normal incidence, n is the order and $\varepsilon_{\max}$ is a chosen constant.

IV. Numerical Results

To validate the method, we have applied this ABC to both radiation and waveguide problems solved in terms of wave potentials in the time domain. The equations are discretized using central finite differences. The auxiliary variables $\vec{X}_1$, $\vec{Y}_1$, $\vec{Z}_1$ are positioned half a cell "after" $\vec{A}$ along the x-, y-, and z-axis, respectively; and $\vec{X}_2$, $\vec{Y}_2$, $\vec{Z}_2$ are at the same locations as $\vec{A}$. Here, we will consider two examples: a dipole in open space and a hollow rectangular waveguide. The problem of the z-directed infinitesimal dipole, which radiates in open space, has two planes of symmetry. Thus, the computational domain is only one octant whose dimensions are ($90\Delta x$, $90\Delta y$, $90\Delta z$), where $\Delta x = \Delta y = \Delta z = 2.5$ mm. The potential is excited by the z-directed current of the dipole, which is a Gaussian pulse in time. The reflection is calculated using the ratio of the reflected and the incident potentials, which have only a z-component, $\vec{A} = \hat{z}A_z$

$$R_{\mathrm{dB}} = 20\log_{10}\left|\frac{\mathcal{F}\left\{A_z^{refl}\right\}}{\mathcal{F}\left\{A_z^{inc}\right\}}\right| \quad (10)$$

where $\mathcal{F}$ denotes the Fourier transform of the respective time-dependent potential. The sampling point is chosen half-way between the excitation point and the PML end so that there is sufficient time guard allowing clear separation of the incident and reflected wave. Identical results are obtained with de-embedding using the incident pulse recorded in a computational volume, whose size is $180\triangle h$. We investigate three types of PML ABCs to terminate the computational domain of the time-domain wave equation. They have different variable profiles. One of them implements the MPML conductivity profile as in [11]. The second one uses the GPML profile [12]. The third absorber is based on the modified profile proposed in (8) and (9). All of them are 20 cells thick; their theoretical reflection coefficient at normal incidence is chosen to be $R_0 = 10^{-4}$; the constant $\varepsilon_{\max}$ is set as $\varepsilon_{\max} = 2$, and the order n defined in (8) and (9) is set to $n = 2$. Their respective reflections are plotted in Fig. 1, which shows that our modification of the PML conductivity profile offers superior performance in terms of both reflection level and frequency bandwidth. In all cases, the observation point is in the dipole's H-plane, halfway from the absorber. The reflections are similar for any other observation point.

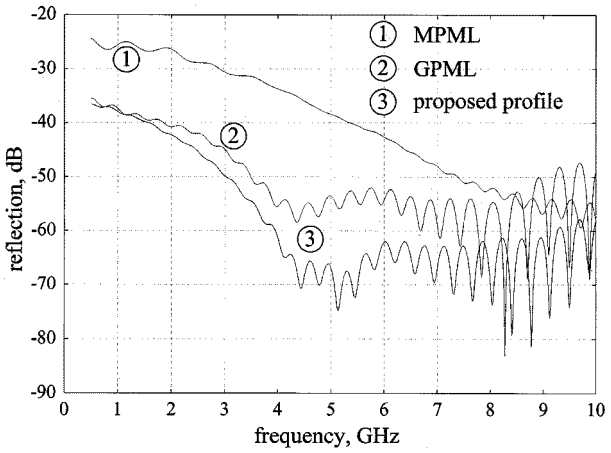

Fig. 1. Spectrum of the reflection in the dipole radiation problem using three different PML conductivity profiles: 1—MPML [11], 2—GPML [12], and 3—current profiles ($N_{\mathrm{PML}} = 20$, $R_0 = 10^{-4}$, $\varepsilon_{\max} = 2$, $n = 2$ in all three cases).

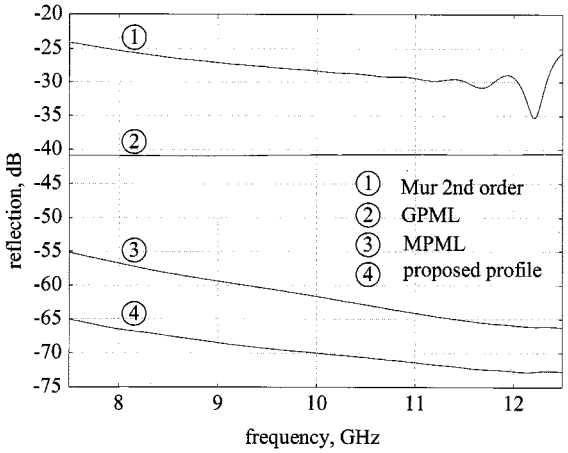

Fig. 2. Spectrum of the reflection in the waveguide problem with different PML conductivity profiles compared to Mur's second order ABC: 1—Mur's second order ABC [14], 2—GPML [12], 3—MPML [11], and 4—current profiles ($N_{\mathrm{PML}} = 8$, $R_0 = 10^{-4}$, $\varepsilon_{\max} = 1$, $n = 2$, in all three PML cases).

The rectangular waveguide has a cross-section of 30 mm by 15 mm. It is excited by a 10 GHz sine waveform modulated by Blackman-Harris window function [13]. The bandlimited excitation has its spectrum in the frequency band from 7.5 GHz to 12.5 GHz. The size of the computational domain is ($350\Delta x$, $30\Delta y$, $15\Delta z$), where $\Delta x = \Delta y = \Delta z = 1$ mm. The ports were terminated by the same three types of PML ABCs as described above and by Mur's second order ABC [14]. The PML is eight cells thick and $R_0 = 10^{-4}$, $\varepsilon_{\max} = 1$, $n = 2$. The reflections as defined in (10) are plotted in Fig. 2. The same low-reflection broadband performance of the proposed modified PML profile is observed.

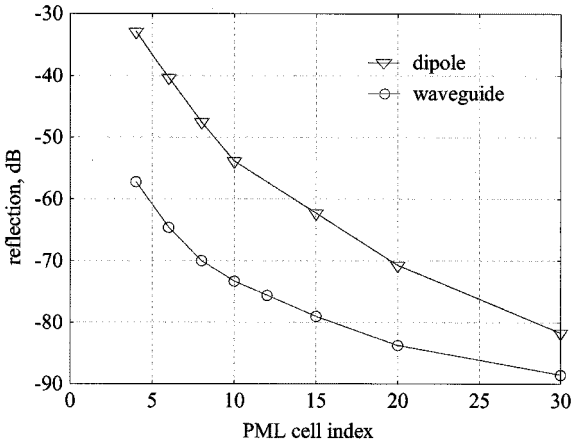

Fig. 3. Dependence of the reflection on the thickness of the PML: dipole—at 8 GHz, waveguide—at 10 GHz ($R_0 = 10^{-4}$, $\varepsilon_{\max} = 1$, $n = 2$).

The dependence of the reflection level on the number of layers in the proposed absorber is shown in Fig. 3 at specific frequencies: 8 GHz for the dipole and 10 GHz for the waveguide ($R_0 = 10^{-4}$, $\varepsilon_{\max} = 1$, $n = 2$ in both examples). However, the curves in the whole frequency band have similar behavior. Generally, one can draw the conclusion that the same thickness of the PML is needed for the termination of the 3-D computational domain of the wave equation compared to the FDTD solution of Maxwell's equations. To achieve a reflection under 0.1% in a broad frequency band, at least 12 PML cells are necessary.

V. Conclusion

In this letter, we propose an efficient PML ABC for the 3-D wave equation in the time domain. It is shown that the conventional PML profiles are not efficient when integrated with the second-order wave equation. Suitable low-reflection broadband PML variable profile is proposed. Its performance is verified in both radiation and waveguide problems. The new profile shows versatility with respect to the geometry and the type of the problem. The current implementation can handle also inhomogeneous dielectrics intersecting the PML boundary. Further implementations include complex structures with metallic inclusions.

References

[1] J. P. Berenger, "A perfectly matched layer for the absorption of electromagnetic waves," *J. Comput. Phys.*, vol. 114, pp. 185–200, 1994.

[2] ——, "Perfectly matched layer for the FDTD solution of wave-structure interaction problems," *IEEE Trans. Antennas Propagat.*, vol. 44, pp. 110–117, Jan. 1996.

[3] W. P. Huang, C. L. Xu, and K. Yokoyama, "The perfectly matched layer boundary condition for modal analysis of optical waveguides: Leaky mode calculations," *IEEE Photon. Technol. Lett.*, vol. 8, pp. 652–654, May, 1996.

[4] J. Tang, K. D. Paulsen, and S. A. Haider, "Perfectly matched layer mesh terminations for nodal-based finite-element methods in electromagnetic scattering," *IEEE Trans. Antennas Propagat.*, vol. 46, pp. 507–516, Apr. 1998.

[5] A. Cuccinotta, G. Pelosi, S. Selleri, L. Vincetti, and M. Zoboli, "Perfectly matched anisotropic layers for optical waveguide analysis through the finite-element beam-propagation method," *Microwave Opt. Technol. Lett.*, vol. 23, pp. 67–69, Feb. 1999.

[6] B. Stupfel and R. Mittra, "Numerical absorbing boundary conditions for the scalar and vector wave equations," *IEEE Trans. Antennas Propagat.*, vol. 44, pp. 1015–1022, July 1996.

[7] D. Zhou, W. P. Huang, C. L. Xu, and D. G. Fang, "The perfectly matched layer boundary condition for scalar finite-difference time-domain method," *IEEE Photon. Technol. Lett.*, vol. 13, pp. 454–456, May 2001.

[8] N. Georgieva, "Construction of solutions to electromagnetic problems in terms of two collinear vector potentials," *IEEE Trans. Microwave Theory Tech.*, vol. 50, Sept. 2002, to be published.

[9] N. Georgieva and Y. Rickard, "The application of the wave potential functions to the analysis of transient electromagnetic fields," in *IEEE MTT-S Int. Symp. Dig.*, vol. 2, June 2000, pp. 1129–1132.

[10] W. C. Chew and W. H. Weedom, "A 3-D perfectly matched medium from modified Maxwell's equations with stretched coordinates," *Microwave Opt. Technol. Lett.*, vol. 7, no. 13, pp. 599–604, 1994.

[11] B. Chen, D. G. Fang, and B. H. Zhou, "Modified Berenger PML absorbing boundary condition for FD-TD meshes," *IEEE Microwave Guided Wave Lett.*, vol. 5, pp. 399–401, Nov. 1995.

[12] J. Fang and Z. Wu, "Generalized perfectly matched layer for the absorption of propagating and evanescent waves in lossless and lossy media," *IEEE Trans. Microwave Theory Tech.*, vol. 44, pp. 2216–2222, Dec. 1996.

[13] F. J. Harris, "On the use of windows for harmonic analysis with the discrete Fourier transform," *Proc. IEEE*, vol. 66, pp. 51–83, Jan. 1978.

[14] G. Mur, "Absorbing boundary conditions for the finite-difference approximation of the time-domain electromagnetic-field equations," *IEEE Trans. Electromagn. Compat.*, vol. EMC-23, pp. 377–382, Apr. 1981.